Accepted Manuscript

Keratinocyte Sonic Hedgehog Up-regulation Drives the Development of Giant Congenital Nevi via Paracrine Endothelin-1 Secretion

Arash Chitsazan, Blake Ferguson, Rehan Villani, Herlina Y. Handoko, Pamela Mukhopadhyay, Brian Gabrielli, Wolter J. Mooi, H. Peter Soyer, Duncan Lambie, Kiarash Khosrotehrani, Grant Morahan, Graeme J. Walker

PII: S0022-202X(17)33158-5

DOI: 10.1016/j.jid.2017.10.032

Reference: JID 1169

To appear in: *The Journal of Investigative Dermatology*

Received Date: 27 July 2017

Revised Date: 21 October 2017

Accepted Date: 23 October 2017

Please cite this article as: Chitsazan A, Ferguson B, Villani R, Handoko HY, Mukhopadhyay P, Gabrielli B, Mooi WJ, Soyer HP, Lambie D, Khosrotehrani K, Morahan G, Walker GJ, Keratinocyte Sonic Hedgehog Up-regulation Drives the Development of Giant Congenital Nevi via Paracrine Endothelin-1 Secretion, *The Journal of Investigative Dermatology* (2017), doi: 10.1016/j.jid.2017.10.032.

Keratinocyte Sonic Hedgehog Up-regulation Drives the Development of Giant Congenital Nevi via Paracrine Endothelin-1 Secretion

Arash Chitsazan[1,2], Blake Ferguson[1], Rehan Villani[2], Herlina Y. Handoko[1], Pamela Mukhopadhyay[1], Brian Gabrielli[3], Wolter J. Mooi[4], H. Peter Soyer[2], Duncan Lambie[2], Kiarash Khosrotehrani[2], Grant Morahan[5], Graeme J. Walker[1].

[1]Drug Discovery Group, QIMR Berghofer Medical Research Institute, Herston, Queensland, Australia.

[2]The University of Queensland Diamantina Institute, Translational Research Institute, Brisbane, Queensland, Australia.

[3]Mater Medical Research Institute, The University of Queensland, Translational Research Institute, Brisbane, Queensland, Australia.

[4]Department of Pathology, Vrije University Medical Center, Amsterdam, Netherlands.

[5]Centre for Diabetes Research, Harry Perkins Institute of Medical Research, Perth, Western Australia, Australia.

Keywords

Cdon, Collaborative Cross, Endothelin-1, Giant Congenital Nevus, Melanocytoma, Melanoma

Corresponding author: Dr Graeme Walker,

QIMR Berghofer Medical Research Institute,

300 Herston Rd, Herston, QLD 4006, Australia.

Tel: +61738453715, Fax: +61738453508

Email: Graeme.Walker@qimrberghofer.edu.au

Abstract

Giant congenital nevi are associated with clinical complications such as neurocutaneous melanosis and melanoma. Virtually nothing is known about why some individuals develop these lesions. We previously identified the sonic hedgehog (Shh) pathway regulator *Cdon* as a candidate nevus modifier gene. Here we validate this by studying *Cdon* knockout mice, and go on to establishment the mechanism by which Shh exacerbates nevogenesis. *Cdon* knockout mice develop blue nevi without the need for somatic melanocyte oncogenic mutation. In a mouse model carrying melanocyte $NRAS^{Q61K}$ we found that strain backgrounds that carry genetic variants that cause increased keratinocyte Shh pathway activity, as measured by Gli1 and Gli2 expression, develop giant congenital nevi. Shh components are also active adjacent to human congenital nevi. Mechanistically, this exacerbation of nevogenesis is driven via the release of the melanocyte mitogen endothelin-1 from keratinocytes. We then suppressed nevus development in mice using Shh and endothelin antagonists. Our work suggests a novel aspect of nevus development whereby keratinocyte cytokines such as endothelin-1 can exacerbate nevogenesis, and provides potential therapeutic approaches for giant congenital nevi. Further, it highlights the notion that germline genetic variation, in addition to somatic melanocyte mutation, can strongly influence the histopathological features of melanocytic nevi.

Introduction

The presence of multiple nevi is the strongest risk factor for development of melanoma (Gandini et al, 2005). Whereas common acquired nevi emanate from the dermo-epithelial junction of the skin, many nevi are dermal or have a dermal component. Congenital nevi are mostly dermal, and observed at birth or in the very young (Sowa et al, 2008; Price et al, 2010). They may be small birthmarks anywhere on the body, large lesions mostly on the head and neck, or giant lesions sometimes covering large areas of body. The latter have an increased risk for transformation melanoma (Zaal et al., 2004). Some patients develop neural melanosis, which carries a poor prognosis, with no effective treatment (Flores-Sarnat et al, 2013). One way to approach understanding the formation of these lesions is to look for natural gene variation that confers susceptibility to their development. But in terms of germline gene variation there are no GWAS or genetic association studies conducted on human giant congenital nevi patients, nor familial studies that might reveal rare mutations

Congenital nevi probably derive from melanocytes that have escaped the developmental route from the neural crest to the skin, and become trapped in the dermis, where they proliferate. Many transgenic mice carrying melanocyte-specific oncogenic mutations develop dermal melanocytic proliferations reminiscent of giant congenital nevi (Shakhova et al, 2012; Pawlikowski et al, 2015). Transgenic *Cdk4*^{R24C}*::Tyr-NRAS*^{Q61K} (hereafter termed *Cdk4::NRAS*) mice begin to develop dermal nevi during the second week after birth (Chai et al., 2014; Chitsazan et al, 2016). Since the corresponding developmental period in which embryonic melanocytes have mostly migrated to the hair bulb is pre-natal in humans, beginning at around 18 weeks (Gleason et al, 2008), and examination of aborted foetuses at this stage have indicated the presence of deep dermal nevi at this stage (Cramer and Fesyuk, 2012), one might expect that the mechanisms promoting escape of melanocytes from the hair follicle to the dermis should be similar in both species. Hence in order to discover genes affecting congenital nevogenesis, we utilised the Collaborative Cross (CC) (Morahan et al, 2008; Welsh et al, 2014), a resource of characterised mouse strains, in conjunction with the *Cdk4:;NRAS* model, to identify a quantitative trait locus (QTL) on mouse chromosome 9 (Chitsazan et al, 2016) influencing nevocyte density. Examination of the founder haplotype coefficients through the linked interval on chromosome 9 showed that the nevus-susceptible strains carried the causal variant derived from the NOD/LtJ founder (hereafter termed NOD). One of the best candidates in this QTL was *Cdon*, a sonic hedgehog (Shh) pathway regulator, which when knocked out in zebrafish results in hyperpigmentation of the dorsal surface (Powell et al, 2015). Shh signalling

is controlled by dependence receptors Cdon and Ptch1 (Delloye-Bourgeois et al, 2013). Their inactivation by Shh removes the inhibition on smoothened (Smo), a positive regulator of Gli transcription factors (Ruiz Altaba, 1997; Taipale et al, 2002; Oro and Higgins, 2003; Ouspenskaia et al, 2016, Brownell et al, 2011). Deregulation of the SHH pathway drives the formation of the keratinocyte-derived skin cancer, basal cell carcinoma (BCC), which are sometimes pigmented. Here we define a cell extrinsic role for the Shh-endothelin1 axis in the development of giant congenital nevi.

Results

Genetic Background Dictates the Histopathology of Melanocytic Hyperplasia

Cdk4::NRAS mice develop dermal nevi by postnatal day 10, from melanocytes escaping the hair follicles (Chitsazan et al, 2016). *Cdk4*$^{R24C/R24C}$*::Tyr-NRAS*$^{Q61K/+}$ males were bred with females from many CC strains to generate progeny heterozygous for *Cdk4* and *NRAS* transgenes. Dorsal skin was collected from >3 progeny of each CC cross, and the density of dermal nevocytes scored from 1 (least dense) to 10 (most dense). The method of scoring each strain for nevus cell density in the dermis is described in Chitsazan et al. (2016). Here we went on to diagnose lesions at each density level according to histopathological criteria for diagnosing human melanocytic hyperplasia. Those with a score of 1-4 were best defined as superficial or deep blue nevi (Figure 1a; Figure S1), a score of 5-6 as deep penetrating nevi, 7 as epitheloid blue nevus, and 8-10 as melanocytoma (Gavriilidis et al, 2013, Zembowicz and Scolyer, 2011). The nevus density score was closely related to depth and histopathological diagnosis (Figure 1b). In general a particular histopathological parameter may be shared by more than one lesion subtype, and we observed a gradation of nevocyte density scores closely, but not perfectly, reflecting nevus subtype (Figures 1c). Despite all mice carrying a melanocyte *NRAS*^{Q61K} mutation making them susceptible to the development of nevi, germ-line genetic variation dramatically alters nevus histopathological presentation.

Validation of a candidate Modifier Gene for Nevus Exacerbation

Previously we identified *Cdon* as candidate nevus modifier gene by studying *Cdk4::NRAS* mice crossed onto many CC strain backgrounds (Chitsazan et al, 2016). We used heterozygous loss of *Cdon*, since homozygous loss is embryonic lethal (Cole and Kraus, 2003). *Cdon*$^{+/-}$ mice (n=4), and not littermate wild type controls (n=3), developed blue nevi in old age. Dermoscopy of the lesions showed a blue hue suggesting nevocyte location in the deep dermis (Figure 2a).

Dendritic and epithelioid melanocytes were present. We also noted the presence of pigmented melanocytes in the telogen bulge region that were not present in wt mice (Figure 2b). Of note, these aged *Cdon*$^{+/-}$ mice had fewer hair follicles than controls (Figure S4). The differences in hair follicle number are unsurprising given the pivotal role of Shh in hair follicle homeostasis (Sato et al, 1999). *Cdon*$^{+/-}$ mice develop dermal nevi without the need for somatic *BRAF* or *NRAS* mutation in melanocytes.

We then assessed the visual appearance of *Cdk4::NRAS* mice carrying the *Cdon*^{NOD} allele (Figure 2c), versus controls carrying the non-NOD allele (by genotyping the *Cdon*^{P456S} mutation). Both cohorts were hyperpigmented, but susceptible mice carrying *Cdon*^{NOD} developed leathery thickenings reminiscent of giant congenital nevi. Dermoscopy of the tail and dorsal skin of resistant mice showed a scattered blue hue on a white background with some small superficial and deep nodules, whereas in the susceptible mice carrying *Cdon*^{NOD} both the deeper nevi and nodules were much larger (Figure 2c). Histologically, the former were blue nevi, while the latter consisted of strings interconnected melanocytomas producing a macroscopic appearance of giant congenital nevus. The formation of leathery lesions can be observed in patients with medium-sized or giant congenital nevi (Figure 2d). The human and murine giant congenital nevi lesions showed other similarities including generalised hyperpigmentation, some large plaques, and ectopic hair growth (hypertrichosis). Inactivation of the Shh pathway in mouse keratinocytes, in conjunction with melanocyte *NRAS*^{Q61K} mutation, produced large leathery melanocytic plaques reminiscent of human giant congenital nevi. Thus, while we do not know that status of the SHH pathway in such individuals, upregulated keratinocyte SHH and EDN1 might be one potential mechanism.

In vivo Activation of Shh Signaling in *Cdk4::NRAS* Mice with Giant Congenital Nevi

To confirm activation of the Shh pathway in strains carrying the *Cdon*^{NOD} variant we stained the mouse skin for Gli1 and Gli2, markers of Shh activation, using multiplexed immunofluorescence (IF) staining with Tyramide-based amplification (Figure 3). We stained dorsal skin from *Cdk4::NRAS* mice with Sox10 (a melanocyte maker) and Gli1 and Gli2 antibodies, to examine protein expression in the vicinity of the early nevi (mice at P10 and P21), and melanocytoma (in adult mice). In *Cdon*^{NOD} strains, at P10, when nevi are beginning to form, Gli proteins were mostly expressed in the hair follicle (Figure 3a). In contrast, in the skin of resistant strains there was low levels Gli expression at P10 (Figures 3b), which was confirmed by quantitating the proportion of Gli1 and Gli2 positive cells in the skin using InForm software (Figures 3e, and 3f). Likewise, in susceptible adult mice with follicles in *telogen*, Gli1 and Gli2 were expressed in a

much higher proportion of cells within the skin than in resistant CC mouse strains (Figure 3c, d. e, f).

In human skin, CDON is expressed mainly in the suprabasal epidermis, and in parts of the hair follicle (Figure S2). In mouse skin also Cdon is expressed in the epidermis and the hair follicle. We stained four human intradermal nevi (Figure 3g and S3a**)** with congenital features including deep extension into the reticular dermis, and peri-appendageal accentuation. CDON was mostly expressed in differentiated keratinocytes in upper epidermis, and in the hair follicle. The expression of GLIs in keratinocytes is consistent with a role for activated SHH in exacerbating human dermal nevus development. In the mouse this effect largely influences the early stages of nevus formation, which occur prenatally in humans. Understanding the temporal development (beginning at ~ 10 days of age), and the skin compartment in which they are first observed (in the superficial dermis adjacent to hair follicles) in our mouse model, provides us with a unique opportunity to better study the mechanisms by which natural genetic variation influences congenital nevi formation.

Linking Keratinocyte Shh Signalling to Development of Dermal Nevi

LDE225, a potent antagonist of the Shh pathway protein Smo, is an FDA-approved drug for topical treatment of BCC (Skvara et al, 2011). We administered this topically in DMSO to the dorsal skin every day from P5 to P10. Skin samples harvested at the end of P10 from drug-treated and control groups were stained for Sox10 (Figure 3h). Whereas at P10 small groups of melanocytes (early nevi) were beginning to form in the control mice, these were not evident in the drug-treated animals. The proportion of Sox10 positive nuclei in the dorsal skin of LDE225-treated mice was significantly lower in the superficial dermis than in controls (Figure 3i). The drug treatment also suppressed melanocyte numbers in the hair bulb suggesting that less melanocytes may be escaping from it (Figure 3i). Thus, drug targeting of Shh pathway activity can significantly suppress nevus formation.

Shh-Edn1 Axis Exacerbates Nevogenesis

Basal cell carcinomas in humans and mice are sometimes pigmented (Chow et al, 2011; Grachtchouk et al, 2003; Moore and Bennett, 2012; Peterson et al, 2015). In mice with keratinocyte-specific inactivation of Ptch1 (Peterson et al, 2015), or activation of other Shh pathway components e.g. Smo (Grachtchouk et al, 2003), Gli2 (Grachtchouk et al, 2000), and

Shh (Ellis et al, 2003), hyperpigmentation is usually evident as pigmented melanocytes within or near BCCs. These transgenics were all generated to study BCC hence the hyperpigmentation phenotypes were generally not described. Where hyperpigmented skin was reported, and adequate published images available, the lesions appeared to be blue nevi (Ellis et al, 2003), which also develop in the Cdon$^{+/-}$ mice.

We set out to ask which genes that influence melanocyte behaviour are over-expressed in the skin of these transgenics? We compared gene expression from RNA sequencing of *Ptch1* knockout epidermis to that of controls. For additional confirmation we used published data from another mouse BCC model (Youssef et al, 2012). In this case YFP-positive keratinocytes were isolated from tamoxifen-treated and control *K14-Cre^{ER}::Rosa-Smo2 (K14-Smo2)* mice, and microarray gene expression analysis performed. In both cases Shh target genes are up-regulated in keratinocytes e.g. *Gli1, Gli2, Ptch1* (Figure 4a). Given that transgenic over-expression of known melanocyte mitogens like hepatocyte growth factor (Hgf), endothelin 3 (Edn3), in murine keratinocytes induces similar melanocytic dermal lesions to that we see in our model (Aoki et al., 2009), we looked for up-regulation of genes encoding secreted cytokines known to be melanocyte mitogens; *Edn1, Edn2, Edn3, Hgf, Fgf, Pomc* (*αMsh* and *Acth*), and *Ngf* (Hirobe, 2005), and *Wnt5a* and *Wnt7b* (Figure 4a). *Edn1* (endothelin 1) (Zhang et al, 2013; Hyter et al, 2013; Urtatiz et al, 2016; Chiriboga et al, 2016) was the only such gene statistically upregulated in both the Ptch1 and Smo mouse model epidermis. By IF staining of mouse dorsal skin we found that Edn1 is expressed in the epidermis and certain cells in the outer root sheath and hair bulb (Figure 4b). We quantitated the expression of Edn1 protein in susceptible and resistant strains at P10. The number of positive cells per mm^2 was significantly higher in the susceptible strains (Figure 4c), suggesting that Edn1 secretion is a plausible mechanism for exacerbation of nevogenesis. We then compared Edn1 expression in WT and aged *Cdon$^{+/-}$* mice with hair follicles in telogen (Figure 4d). Quantitation of the proportion of cells positive for Edn1 showed that the *Cdon$^{+/-}$* mice express more of this cytokine than wild type mice (Figure 4e). To confirm the functional effect of Edn1 in exacerbating nevogenesis, we utilized an inhibitor of the Edn1 receptor, Bosentan. Daily treatments of *Cdk4-NRAS* mice (from P5 to P10 intraperitoneally and topically) with Bosentan significantly reduced the appearance of blue nevi in the superficial dermis (Figures 4f and 4g), and the hair follicle (Figure 4f and 4h).

Discussion

Although *NRAS*^{Q61K} mutation is the major somatic mutation carried in giant congenital nevi, virtually nothing else is known about the mechanism of formation of these lesions. Despite the evolutionary differences in the pigmentary system between species (mouse melanocytes are usually limited to hair follicles whereas in humans they are also in the epidermis), virtually all genes involved in regulating mouse melanocyte behaviour (i.e. pigmentation) are relevant in humans (Walker et al, 2011). Given that we have gone to great lengths to diagnose the murine nevi precisely according to the histopathological criteria used for human nevi, and shown that the pathway we have discovered is active in the epidermis adjacent to human congenital nevi, the cell extrinsic mechanism we have delineated could be involved in the formation of human nevi. It is not known whether germline *CDON* variants influence the development of human congenital nevi, but our findings enable us to postulate that variants in any gene that results in up-regulation of a pathway that increases expression of a secreted keratinocyte cytokine that is a melanocyte mitogen, could be a candidate.

A role for paracrine Edn1 driving nevogenesis seems uncontroversial. It is a mitogen for human melanocytes in culture (Imokawa et al., 1992) and in human skin explants (Takeo et al., 2016), and is involved in wound-induced melanocyte activation (Park et al, 2015). Edn1, along with Edn2 and Edn3, are mostly active only in *anagen*, or growth phase of the hair cycle, when they assist either to activate melanocyte stem cells, and/or to assist in migration of melanocytes to the hair bulb (Rabbani et al, 2011; Takeo et al, 2016; Mort et al, 2015). Hence under stress such as increased endothelin secretion or the presence of a NRAS or BRAF mutation it is unsurprising that melanocytes escape their follicular niches and congregate in the dermis as nevi. Edn1 binds to the melanocyte Ednrb receptor and stimulates signalling through Gnaq/Gna11 and subsequently the MAPK pathway (Figure 5). *GNAQ* is somatically mutated in ~80% of human blue nevi, suggesting that signalling through it is important in dermal nevus development, and mice expressing an activated *Gnaq* mutant in their melanocytes exhibit essentially the same phenotype in terms of dermal melanocytic nevi that we observe in our model with activated keratinocyte Shh (Huang et al., 2015). Perhaps SHH-EDN1 signalling acts as a rheostat, via melanocyte EDN1-GNAQ-MAPK, in exacerbating blue nevi to form very large or giant nevi (Figure 5).

SHH is normally associated with BCC. *PTCH1* is frequently mutated in BCC-prone patients, and the SHH pathway is mutated somatically in BCC (Tang et al., 2010; Briscoe and Therond, 2013). Notably, the mouse strains carrying the *Cdon*^{NOD} variant do not develop BCC,

presumably since the associated keratinocyte Shh up-regulation is relatively subtle. But one would expect BCCs to be pigmented, and many are, with melanocytes unusually located around the edges or within the lesion. EDN1 is highly expressed adjacent pigmented, but not non-pigmented human BCCs (Lan et al, 2005). Since 80% of Asian, but only 3% of Caucasian BCCs (Moore and Bennett, 2012; Chow et al, 2011), it is likely that modifier alleles that differ between these ethnic backgrounds modulate the SHH-EDN1 axis. However murine models with keratinocyte-specific deregulation of Shh components e.g. *Shh* (Ellis et al, 2003), *Ptch1* (Peterson et al, 2015), *Smo* (Grachtchouk et al, 2003) and *Gli2* (Grachtchouk et al, 2000), all exhibit melanocyte hyperplasia.

An important message is the notion that different genes act at different stages of tumor progression. We show (Figure 1c) that the strains carrying the $Cdon^{NOD}$ allele and upregulated keratinocyte Shh components are not necessarily more prone to the development of melanoma, although the nevi are much larger. Since the transformation of an individual nevus (of which there are >10,000 per mouse on an FVB strain background) is extremely low (a 0.04% probability that a nevus will convert to melanoma; Chai et al, 2014), it must be modified by epigenetic, or other genetic background effects that are yet been elucidated.

Our strategy using mouse models could be helpful in gaining insights into genetic background influences in other rare diseases. Giant congenital nevi are only seen in about 1/20,000 births, and no genetic studies have been performed on large case-control cohorts. But they can be disfiguring, covering significant parts of the body surface, and with a high propensity to convert to melanoma. They are not always stable. Satellite lesions can form, and neural melanosis sometimes becomes manifest in these patients. Studying human lesions post-natally does not tell us how they are formed. In years to come germ-line DNA from large enough cohorts may become available for genome wide association studies into susceptibility. But not being a common disease it will be difficult to attract traditional research funding. To confirm our hypothesis that keratinocyte cytokines may feed the formation of giant nevi would entail sensitive gene expression and or immunohistochemical studies of representative skin samples from perhaps hundreds of patients and ethnic matched controls, again a difficult study to realize.

Targeting keratinocyte cytokines might provide hope for a drug therapy by which giant nevi could be controlled, or even reversed, since they can spontaneously regress (Arpaia et al, 2005; Nath et al, 2011; Cusak et al, 2009). Surgical excision is the gold standard treatment for most cutaneous tumours. But topical treatments are now available for solar keratosis and *in situ*

squamous and basal cell carcinomas (e.g. fluorouracil, imiquimod, Picato gels), lesions previously only removed by excision. The same may eventually be true for large/giant nevi. Topical treatment of pigmented BCCs with the SMO antagonist LDE225, and Bosentan an inhibitor of Edn signalling, which we used in our study to suppress the development of dermal nevi, results in the disappearance of the associated melanocytosis.

Methods

Mice and Phenotyping

Mouse breeding and screening for nevus density modifier gene: By breeding *Cdk4*$^{R24C/R24C}$*::Tyr-NRAS*$^{Q61K/+}$ males with females from 70 CC strains. Experiments were undertaken with institute animal ethics approval (A98004M). *Cdon* knockout mice were kindly provided by Robert S. Krauss (Icahn School of Medicine at Mount Sinai, NY). Collaborative Cross mouse strains were provided by Grant Morahan (Harry Perkins Institute of Medical Research, Perth). By breeding *Cdk4*$^{R24C/R24C}$*::Tyr-NRAS*$^{Q61K/+}$ males (FVB background) with CC females we generated progeny heterozygous for *Cdk4* and *NRAS* (Chitsazan 2016). At P10 small nests of melanocytic cells (nevi) appear within the superficial dermis around hair follicles (Chai et al, 2013). Nevi are completely formed by P40.

Human study

Experiments were undertaken with the University of Queensland Human Research Ethics Committee A & B approval (approval number 2011001201/HREC/11/QPAH/363).

RNA Sequencing

Four weeks after tamoxifen injection, epidermal cells of *K14-CreER::Ptch1*$^{fl/fl}$ and control mice were recovered by digestion and flow sorting of EPCAM+ epidermal cells. RNA was isolated using RNeasy Kit and libraries generated with Illumina mRNA kit. Sequencing was performed using Ilumina HiSeq chemistry, with 50bp single reads. The RNA-seq samples were mapped to mouse genome MM10 using TopHat2, then mapped reads for each gene counted for every sample using HT-Seq. We used EdgeR and DEseq to estimate the significance of differential expression between groups.

Haematoxylin and Eosin Staining Protocol

Slides from formalin-fixed paraffin-embedded blocks were dewaxed and stained with haematoxylin and eosin using Leica autostainer XL.

Dermoscopy of Mouse Skin

After shaving to remove hair, clinical images were acquired with a digital camera (Canon PowerShot G10; Canon, Tokyo, Japan). Detailed macroscopic images were acquired with the same camera equipped with a dermoscopic attachment (Dermlite©, 3Gen, USA).

Multiplexed Fluorescent Immunohistochemistry with Tyramide Signal Amplification

Sections from paraffin-embedded lesions were dewaxed and treated with Dako low pH antigen retrieval solution at 100^0C for 15 minutes. Endogenous peroxidase activity was quenched in 3% H_2O_2, and sections blocked with 5% bovine serum albumin. Primary Sox10 (sc-17342), Gli1 (ab151796), Gli2 (AF3635), Cdon (sc-134837) and Edn1 (ab117757) antibodies were applied, followed by the appropriate secondary antibodies. After washing, the signal was amplified using Perkin Elmer Tyramide amplificiation kit (FITC, CY3, CY3.5, CY5), slides were washed, counterstained with DAPI, and coverslipped using DAKO mounting medium. Slides were scanned using the Vectra spectral imaging system (PerkinElmer). Images were scanned at at 4X magnification. Multispectral images (MSI) were captured using *Phenochart* software and scanned from 420 nm to 720 nm using Vectra 3.1 Automated quantitative pathology imaging system. Three MSIs per sample was analysed using *InForm* analysis software. Positive cells were segmented and counted per 20X magnification field.

LDE225 Treatment

To generate high nevus count mice we crossed NOD X Cdk4$^{R24C/R24C}$::Tyr-NRAS^{Q61K} transgenics. We topically treated the dorsal area with LDE225-DMSO (10 mg/ml, Selleck Chemicals) every day from P5 to P10 (with skin harvested at P10). Controls were treated with DMSO alone. Skin was harvested from drug treated and control groups (n=21) stained for Sox10 and slides digitised with an Aperio AT-Turbo Brightfield slide scanner. Sox10 positive nuclei count was determined using the Aperio IHC nuclear algorithm V8.001, and nuclear staining stratified into three intensities (1+ to 3+). We scored the number of strongly positive nuclei (3+) per 2 mm^2 section.

Bosentan Hydrate Treatment

To generate nevus-susceptible mice crossed NOD mice with Cdk4$^{R24C/R24C}$::Tyr-NRAS^{Q61K} transgenics. Pups were both injected intraperinatally with Bosentan hydrate-DMSO (10mM/1mL in DMSO, Selleck Chemicals) every day from P5 to P10 (skin harvested at P10). Controls were treated with DMSO. Skin was harvested from drug-treated and control groups (n=14). H&E-stained slides were digitized with Aperio AT-Turbo Brightfield slide scanner, and intensity of

pigmented cells analysed with Aperio-V9 software. We quantitated to intensity of strongly positive cells.

Conflict of interest

The authors state no conflict of interest.

Acknowledgments

We thank members of the Oncogenomics laboratory (QIMR Berghofer Medical Research Institute), for helpful comments. We are grateful to Artur Zembowicz for diagnosis of melanocytic lesions, Brandon Wainwright and Kerstin Zoidl for their critiques of the manuscript. Thanks to Clay Winterford for assistance with multiplex-IHC set up, Nigel Waterhouse and Tam Nguyen for assistance with microscopy, and Sang-Hee Park for histology sample preparation. We thank Robert Krauss and Mingi Hong for kindly providing *Cdon* knockout mice. We thank Geniad Pty Ltd for generously providing CC mice. This work was supported by Melanoma Research Alliance, Washington, DC, USA, and the Cancer Council of Queensland, Australia.

References

Aoki H, Yamada Y, Hara A, Kunisada T. 2009. Two distinct types of mouse melanocyte: differential signaling requirement for the maintenance of non-cutaneous and dermal versus epidermal melanocytes. *Development* 136: 2511-21

Arpaia N, Cassano N, Filotico R, Laricchia F, Vena GA. 2005. Unusual clinical presentation of regression in a congenital melanocytic nevus. *Dermatol Surg* **31**: 471-473.

Briscoe J, Therond PP. 2013. The mechanisms of Hedgehog signalling and its roles in development and disease. *Nat Rev Mol Cell Biol* **14**: 416-429.

Brownell I, Guevara E, Bai CB, Loomis CA, Joyner AL.2011. Nerve-derived sonic hedgehog defines a niche for hair follicle stem cells capable of becoming epidermal stem cells. *Cell Stem Cell* **8**: 552-65.

Chai E, Ferguson B, Prow T, Soyer P, Walker G. 2014. Three-dimensional modelling for estimation of nevus count and probability of nevus-melanoma progression in a murine model. *Pigment Cell Melanoma Res* **27**: 317-319.

Chiriboga L, Meehan S, Osman I, Glick M, de la Cruz G, Howell BS, et al. 2016. Endothelin-1 in the tumor microenvironment correlates with melanoma invasion. *Melanoma Res* **26**: 236-244.

Chitsazan A, Ferguson B, Ram R, Mukhopadhyay P, Handoko HY, Gabrielli B, et al. 2016. A mutation in the Cdon gene potentiates congenital nevus development mediated by NRAS(Q61K). *Pigment Cell Melanoma Res* **29**: 459-464.

Chow VL, Chan JY, Chan RC, Chung JH, Wei WI. 2011. Basal cell carcinoma of the head and neck region in ethnic chinese. *Int J Surg Oncol* **2011**: 890908.

Cole F, Krauss RS. 2003. Microform holoprosencephaly in mice that lack the Ig superfamily member Cdon. *Curr Biol* **13**: 411-415.

Cramer S, Fesyuk A. 2012. On the Development of Neurocutaneous Units—Implications for the Histogenesis of Congenital, Acquired, and Dysplastic Nevi. *Am J Dermatopathol* 34: 60-81.

Cusack C, Warde D, Lynch W, McDermott M, Watson R. 2009. Dramatic spontaneous regression of a medium-sized congenital melanocytic naevus. *Clin Exp Dermatol* **34**: e34-36.

Delloye-Bourgeois C, Gibert B, Rama N, Delcros JG, Gadot N, Scoazec JY, et al. 2013. Sonic Hedgehog promotes tumor cell survival by inhibiting CDON pro-apoptotic activity. *PLoS Biol* **11**: e1001623.

Ellis T, Smyth I, Riley E, Bowles J, Adolphe C, Rothnagel JA, Wicking C, Wainwright BJ. 2003. Overexpression of Sonic Hedgehog suppresses embryonic hair follicle morphogenesis. *Dev Biol* **263**: 203-215.

Flores-Sarnat L. 2013. Neurocutaneous melanocytosis. *Handb Clin Neurol* **111**: 369-388.

Gandini S, Sera F, Cattaruzza MS, Pasquini P, Zanetti R, Masini C, Boyle P, Melchi CF. 2005. Meta-analysis of risk factors for cutaneous melanoma: III. Family history, actinic damage and phenotypic factors. *Eur J Cancer* **41**: 2040-2059.

Gavriilidis P, Michalopoulou I, Chatzikakidou K, Nikolaidou A. 2013. Pigmented epithelioid melanocytoma: a new concept encompassing animal-type melanoma and epithelioid blue nevus. *BMJ Case Rep* **2013**: 2013.

Gleason BC, Crum CP, Murphy GF. 2008. Expression patterns of MITF during human cutaneous embryogenesis: evidence for bulge epithelial expression and persistence of dermal melanoblasts. *J Cutan Pathol* **35**: 615–22.

Grachtchouk M, Mo R, Yu S, Zhang X, Sasaki H, Hui CC, Dlugosz AA. 2000. Basal cell carcinomas in mice overexpressing Gli2 in skin. *Nat Genet* **24**: 216-217.

Grachtchouk V, Grachtchouk M, Lowe L, Johnson T, Wei L, Wang A, et al. 2003. The magnitude of hedgehog signaling activity defines skin tumor phenotype. *Embo j* **22**: 2741-2751.

Hirobe T. (2005). Role of keratinocyte-derived factors involved in regulating the proliferation and differentiation of mammalian epidermal melanocytes. *Pigment Cell Res* 18: 2-12.

Huang JL, Urtatiz O, Van Raamsdonk CD. 2015. Oncogenic G Protein GNAQ Induces Uveal Melanoma and Intravasation in Mice. *Cancer Res* 75: 3384-97.

Hyter S, Coleman DJ, Ganguli-Indra G, Merrill GF, Ma S, Yanagisawa M, Indra AK. 2013. Endothelin-1 is a transcriptional target of p53 in epidermal keratinocytes and regulates ultraviolet-induced melanocyte homeostasis. *Pigment Cell Melanoma Res* **26**: 247-258.

Imokawa G, Yada Y, Miyagishi M. 1992. Endothelins secreted from human keratinocytes are intrinsic mitogens for human melanocytes. *J Biol Chem* **267**: 24675-80.

Lan CC, Wu CS, Cheng CM, Yu CL, Chen GS, Yu HS. 2005. Pigmentation in basal cell carcinoma involves enhanced endothelin-1 expression. *Exp Dermatol* **14**: 528-34.

Moore MG, Bennett RG. 2012a. Basal cell carcinoma in asians: a retrospective analysis of ten patients. *J Skin Cancer* **2012**: 741397.

Morahan G, Balmer L, Monley D. 2008. Establishment of "The Gene Mine": a resource for rapid identification of complex trait genes. *Mamm Genome* **19**: 390-393.

Mort RL, Jackson IJ, Patton EE. 2015. The melanocyte lineage in development and disease. *Development* 142: 620–632.

Nath AK, Thappa DM, Rajesh NG. 2011. Spontaneous regression of a congenital melanocytic nevus. *Indian J Dermatol Venereol Leprol* **77**: 507-510.

Oro AE, Higgins K. (20030). Hair cycle regulation of Hedgehog signal reception. *Dev Biol* **255**: 238-48.

Ouspenskaia T, Matos I, Mertz AF, Fiore VF, Fuchs E. 2016. WNT-SHH Antagonism Specifies and Expands Stem Cells prior to Niche Formation. *Cell* **164**: 156-169.

Park PJ, Lee TR, Cho EG. 2015. Substance P stimulates endothelin 1 secretion via endothelin-converting enzyme 1 and promotes melanogenesis in human melanocytes. *J Invest Dermatol* **135**: 551-559.

Patel AB, Harting MS, Smith-Zagone MJ, Hsu S. 2008. Familial basaloid follicular hamartoma: a report of one family. *Dermatol Online J* **14**: 14.

Pawlikowski JS, McBryan T, van Tuyn J, Drotar ME, Hewitt RN, Maier AB, et al. 2013. Wnt signaling potentiates nevogenesis. *Proc Natl Acad Sci U S A* **110**: 16009-16014.

Peterson SC, Eberl M, Vagnozzi AN, Belkadi A, Veniaminova NA, Verhaegen ME, et al. 2015. Basal cell carcinoma preferentially arises from stem cells within hair follicle and mechanosensory niches. *Cell Stem Cell* **16**: 400-412.

Powell DR, Williams JS, Hernandez-Lagunas L, Salcedo E, O'Brien JH, Artinger KB. 2015. Cdon promotes neural crest migration by regulating N-cadherin localization. *Dev Biol* **407**: 289-299.

Price HN, Schaffer JV. 2010. Congenital melanocytic nevi-when to worry and how to treat: Facts and controversies. *Clin Dermatol* **28**: 293-302.

Rabbani P, Takeo M, Chou W, Myung P, Bosenberg M, Chin L, et al. (2011). Coordinated activation of Wnt in epithelial and melanocyte stem cells initiates pigmented hair regeneration. *Cell* **145**: 941-55.

Ruiz i Altaba A. 1997. Catching a Gli-mpse of Hedgehog. *Cell* **90**: 193-196.

Sato N, Leopold PL, Crystal RG. 1999. Induction of the hair growth phase in postnatal mice by localized transient expression of Sonic hedgehog. *J Clin Invest* **104**: 855-864.

Shakhova O, Zingg D, Schaefer SM, Hari L, Civenni G, Blunschi J, et al. 2012. Sox10 promotes the formation and maintenance of giant congenital naevi and melanoma. *Nat Cell Biol* **14**: 882-890.

Skvara H, Kalthoff F, Meingassner JG, Wolff-Winiski B, Aschauer H, Kelleher JF, et al. 2011. Topical treatment of Basal cell carcinomas in nevoid Basal cell carcinoma syndrome with a smoothened inhibitor. *J Invest Dermatol* **131**: 1735-1744.

Sowa J, Kobayashi H, Ishii M, Kimura T. 2008. Histopathologic findings in Unna's nevus suggest it is a tardive congenital nevus. *Am J Dermatopathol* **30**: 561-566.

Taipale J, Cooper MK, Maiti T, Beachy PA. 2002. Patched acts catalytically to suppress the activity of Smoothened. *Nature* **418**: 892-897.

Takeo M, Lee W, Rabbani P, Sun Q, Hu H, Lim CH, et al. (2016). EdnrB Governs Regenerative Response of Melanocyte Stem Cells by Crosstalk with Wnt Signaling. *Cell Rep* **15**: 1291-302.

Tang T, Tang JY, Li D, Reich M, Callahan CA, Fu L, Yauch RL, Wang F, Kotkow K, Chang KS et al. 2011. Targeting superficial or nodular Basal cell carcinoma with topically formulated small molecule inhibitor of smoothened. *Clin Cancer Res* **17**: 3378-3387.

Urtatiz O, Van Raamsdonk CD. 2016. Gnaq and Gna11 in the Endothelin Signaling Pathway and Melanoma. *Front Genet* **7**: 59.

Walker GJ, Soyer HP, Terzian T, Box NF. 2011. Modelling melanoma in mice. Pigment Cell *Melanoma Res* **24**: 1158-76.

Welsh CE, Miller DR, Manly KF, Wang J, McMillan L, Morahan G, et al. 2012. Status and access to the Collaborative Cross population. *Mamm Genome* **23**: 706-712.

Youssef KK, Lapouge G, Bouvree K, Rorive S, Brohee S, Appelstein O, et al. 2012. Adult interfollicular tumour-initiating cells are reprogrammed into an embryonic hair follicle progenitor-like fate during basal cell carcinoma initiation. *Nat Cell Biol* **14**: 1282-1294.

Zaal LH, Mooi WJ, Sillevis Smitt JH, van der Horst CM. 2004. Classification of congenital melanocytic naevi and malignant transformation: a review of the literature. *Br J Plast Surg* **57**: 707-719.

Zembowicz A, Scolyer RA. 2011. Nevus/Melanocytoma/Melanoma: an emerging paradigm for classification of melanocytic neoplasms? *Arch Pathol Lab Med* **135**: 300-306.

Zhang P, Liu W, Yuan X, Li D, Gu W, Gao T. 2013. Endothelin-1 enhances the melanogenesis via MITF-GPNMB pathway. *BMB Rep* **46**: 364-369.

Figure legends

Figure 1. Comparison of murine and human melanocytic lesions. (a) The inner ring shows representative images of H&E staining of murine melanocytic lesions at each nevocyte density score (1-10). The outer circle shows representative images of H&E staining of corresponding human melanocytic lesions. Scale bars = 100 µm. (b) Distribution of 70 CC strains based on their nevocyte density score and histopathological diagnosis. SBN: Superficial blue nevus, DBN: Deep blue nevus, DPN: Deep penetrating nevus, EBN: Epithelioid blue nevus and M: Melanocytoma. (c) Heat map of pigmentation in megapixel per 20X field of digitized mouse skin from 40 pigmented CC strains bearing *Cdk4::NRAS* and their relevant 1-10 nevocyte density score.

Figure 2. Giant congenital nevus is composed of interconnected melanocytomas. (a) Lesions in *Cdon*$^{+/-}$ mice. By dermoscopy blue coloration is due to dermal melanocytes (blue nevus). H&E shows dermal dendritic melanocytes (yellow arrow), while the white arrow shows dermal epithelioid melanocytes. (b) Normal telogen skin from wild type and *Cdon*$^{+/-}$ mice, showing ectopic pigmentation and higher density of hair follicles in wild type. (c) Visual appearance of dorsal surface of susceptible *Cdk4::NRAS::Cdon*$^{NOD/+}$ mouse (right), at 8 months of age, versus a resistant *Cdk4::NRAS::Cdon*$^{+/+}$ (+/+ = wild type) mouse (left), at 24 months, with dermoscopic images of tail and dorsal skin, and H&E staining of dorsal skin. Both mice are hyperpigmented, but the animal carrying the *Cdon*^{NOD} allele exhibits a large thick giant congenital nevus-like lesion covering the majority of the dorsal surface. All Scale bars = 300 µm. (d) Large human congenital nevus. Red box shows large hyperpigmented plaque within nevus area. Patients provided permission for publication of their images.

Figure 3. Upregulation of Gli in keratinocytes potentiates nevogenesis. Images of 4-plex fluorescent immunohistochemistry with Tyramide signal amplification using Sox10/Gli1/Gli2 antibodies. Samples are of dorsal skin. (a-d) The magnification of images in Figure 4a-4d are the same. Images show susceptible *Cdk4::NRAS::Cdon*$^{NOD/+}$ mice and resistant *Cdk4::NRAS::Cdon*$^{+/+}$ mice at P10 and adulthood. Yellow arrows denote melanocytoma. (e and f) Proportion of Gli1 and Gli2-positive cells per mm^2 in dorsal skin from susceptible and resistant mouse strains at P10 (n=10), P21 (n=10) and adulthood (n=21), quantitated using InForm software (p-values calculated using two-tailed T test, ****=p<0.0001). Scale bars = 60 µm. (g) Human congenital nevus expressing Shh pathway components. Scale bars = 800 µm. (h) Sox10 staining of dorsal skin from susceptible *Cdk4::NRAS::Cdon*$^{NOD/+}$ mice treated with

LDE225 versus (control left panel). Red dotted line denotes superficial blue nevus. Blue arrows denote melanocytes located ectopically in, and at risk of escape from, the hair bulb. Graphs to the right show Sox10-positive nuclei counts in hair follicle bulb (i) at 40X, and the superficial dermis (j), at 20X magnification, of LDE225-treated mice (n=11) and controls (n=10). Cells quantitated using the nuclear staining algorithm of the Aperio™. Scale bars = 60 μm. ****=p<0.0001, **=p<0.007.

Figure 4. Mechanism of exacerbation of nevogenesis. (a) Relative gene expression (Log fold change) in tamoxifen-induced versus control *K14-Ptch1* and *K14CREER/Rosa-SmoM2* epidermis. Differences significant except where marked (n.s=p> 0.05). (b) Expression of Edn1 in P10 anagen skin from *Cdk4::NRAS* mice carrying the $Cdon^{NOD}$ variant. (c) Quantitative protein expression analysis of Edn1 in susceptible $Cdk4::NRAS::Cdon^{NOD/+}$ (n=14 mice) versus a resistant $Cdk4::NRAS::Cdon^{+/+}$ (+/+ denotes wild type at *Cdon*) (n=7), as measured with InForm software (p=value calculated using the two-tailed T test (****= p<0.0001). (d) Edn1 expression in adult WT versus $Cdon^{+/-}$ mouse skin in telogen. (e) Quantitative protein expression analysis of Edn1 in adult WT (n=3) versus $Cdon^{+/-}$ (n=4). (**= p<0.005). (f) Images of H&E staining of dorsal skin from control and Bosentan (an endothelin receptor inhibitor)-treated $Cdk4::NRAS::Cdon^{NOD/+}$ mice. Yellow arrowheads indicate blue nevi. White asterisks denote hair bulb filled with melanocytes in control but not Bosentan-treated mice. Graphs at right show pigmentation level in the dermis (g), and hair follicles (h) of control (n=7) and Bosentan-treated $Cdk4::NRAS::Cdon^{NOD/+}$ mice. There was significantly more pigmentation in control skin (two-tailed T test, **= p<0.001), ****= p<0.0001). All Scale bar = 60 μm.

Figure 5. Model of nevus exacerbation. Proposed mechanism of action of the Cdon-Shh-Edn1 axis, exacerbating nevogenesis. Panel to the left depicts low innate Shh signaling activity in $Cdk4::NRAS::Cdon^{+/+}$ resistant mouse strain ($Cdon^{+/+}$), where $NRAS^{Q61K}$ is the sole driver of nevogenesis. This leads to the formation of blue nevi. In $Cdk4::NRAS::Cdon^{NOD/+}$ mice with high innate Shh signaling, the Shh-Edn1 axis is activated by the $Cdon^{NOD}$ variant. Upregulation and secretion of Edn1 from keratinocytes activates the Ednrb-Gnaq/Gna11 complex, which in turn augments the effect of $NRAS^{Q61K}$ on MAPK, resulting in the formation of melanocytoma (right panel). Targeting of the Cdon-Shh-Edn1 axis using Shh and endothelin pathway antagonists (LDE225 and Bosentan respectively) suppresses nevogenesis.

Suppl. Figure 1. Histopathological variation of melanocytic lesions with *Cdk4::NRAS* mutation. (a) Images of H&E staining of superficial and deep blue nevus in mouse and human.

Nevocytes are comprised of pigmented dendritic cells having wedge shape architecture. (b) Images of H&E staining of mouse and human deep penetrating nevus. These lesions appear in deep dermis, superficial hypodermis, or adjacent to hair follicle bulb area. Pigmented balloon cell-like nevocytes sometimes appear in these lesions. Scale bars = 100 um. (c) Images of H&E staining of mouse non-bleached and bleached epithelioid blue nevus (left) and human epithelioid blue nevus (right). Scale bars = 400 µm. (d) Images of H&E staining of mouse non-bleached and bleached murine melanocytoma (left) and human melanocytoma (right). These lesions contain 3 cell types: dendritic cells, heavily pigmented balloon cells and epithelioid cells. Scale bars = 400 µm.

Supplementary Figure 2. CDON expression in non-lesional human and mouse skin IF staining of CDON in normal human (a) and mouse skin (b). CDON expression is mainly detected in the upper layer of epidermis and in the hair follicles. Scale bar = 100 µm.

Supplementary Figure 3. SHH activity in human dermal nevus and mouse melanocytoma (a) Three-Plex immunofluoresence with tyramide signal amplification (3Plex-TSA) of SOX10, CDON and GLI1 in human dermal nevus with congenital features. CDON is mainly expressed in keratinocytes of epidermis, hair follicle. CDON expression and GLI1 overlap follows similar pattern**.** Scale bars = 300 µm. (b) 3Plex-TSA of adult NOD mouse melanocytoma with Sox10-Cdon-Gli1. Murine lesion shows similar high Shh signalling. Scale bars = 100 µm.

Supplementary Figure 4. Alopecia is observed in high Shh signalling strains (a) H&E images of dorsal skin from wild type and *Cdon* heterozygous knockout littermates. Lower panels, H&E images of dorsal skin from *Cdk4::NRAS*+CC progeny mice on nevus-resistant and susceptible strain backgrounds respectively. Scale bars = 300 µm. (b) Average count per strain of hair follicles per 1.5mm of dorsal skin (WT, n=4, susceptible strains, n=8, wt, resistant strains, n=8, $Cdon^{+/-}$, n= 5). Statistical comparisons performed with a T-=test, ***=p<0.001, **=p<0.01, *=p<0.05

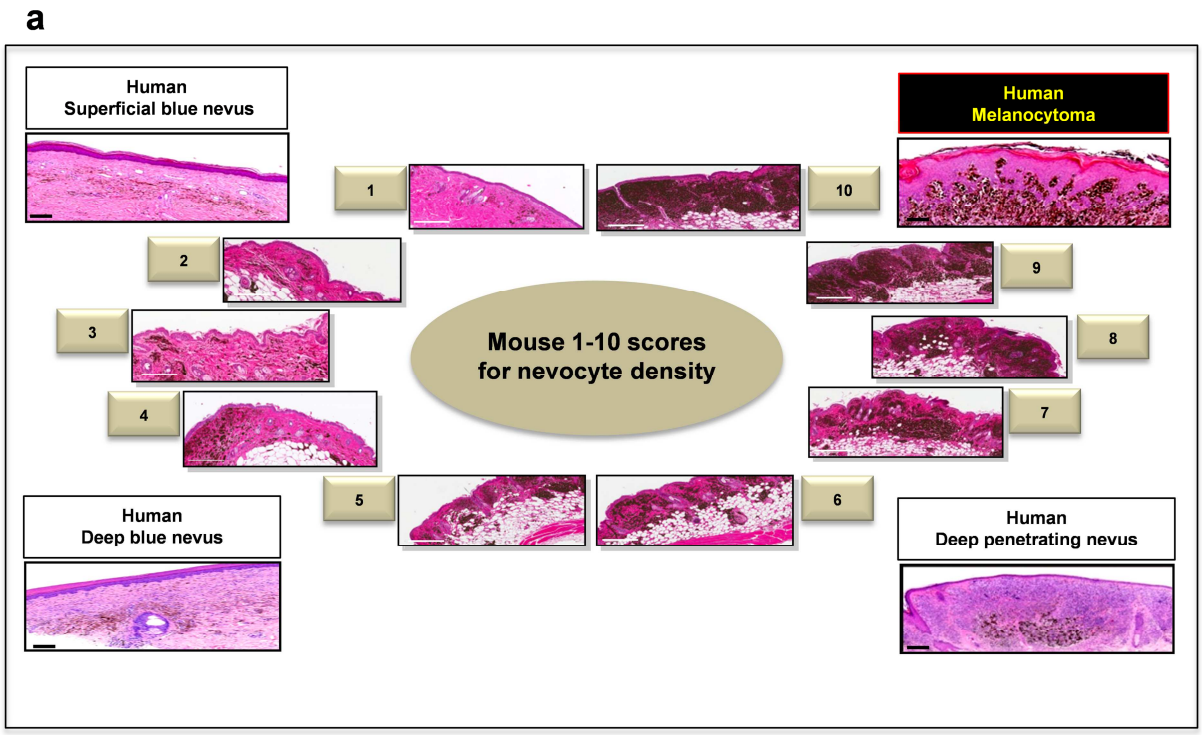
a
Human
Superficial blue nevus
Human
Melanocytoma
1
10
2
9
3
8
4
7
5
6
Mouse 1-10 scores
for nevocyte density
Human
Deep blue nevus
Human
Deep penetrating nevus

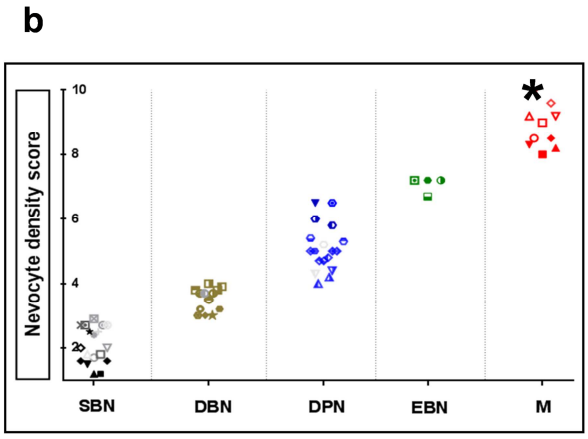
b
Nevocyte density score
10
8
6
4
2
SBN
DBN
DPN
EBN
M
*

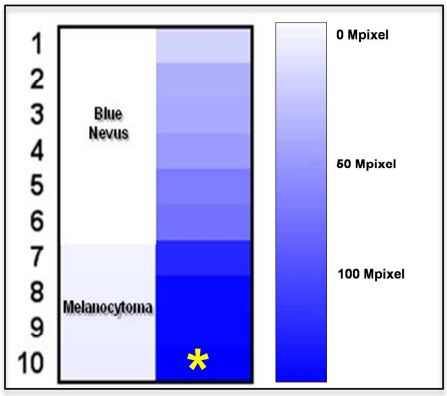
c
1
2
3
4
5
6
7
8
9
10
Blue
Nevus
Melanocytoma
*
0 Mpixel
50 Mpixel
100 Mpixel

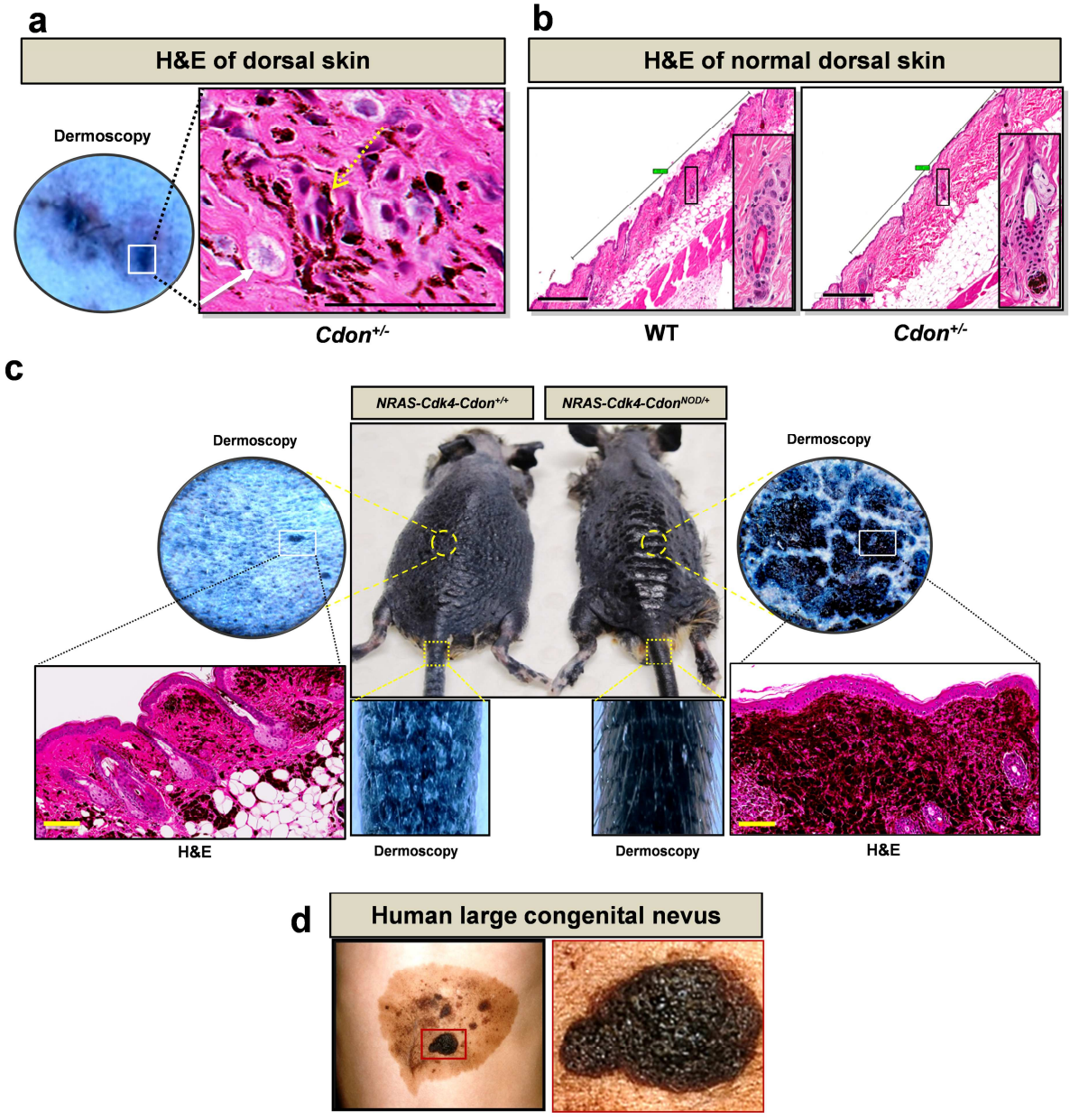
a
H&E of dorsal skin
Dermoscopy
Cdon+/-
b
H&E of normal dorsal skin
WT
Cdon+/-
c
NRAS-Cdk4-Cdon+/+
NRAS-Cdk4-CdonNOD/+
Dermoscopy
Dermoscopy
H&E
Dermoscopy
Dermoscopy
H&E
d
Human large congenital nevus

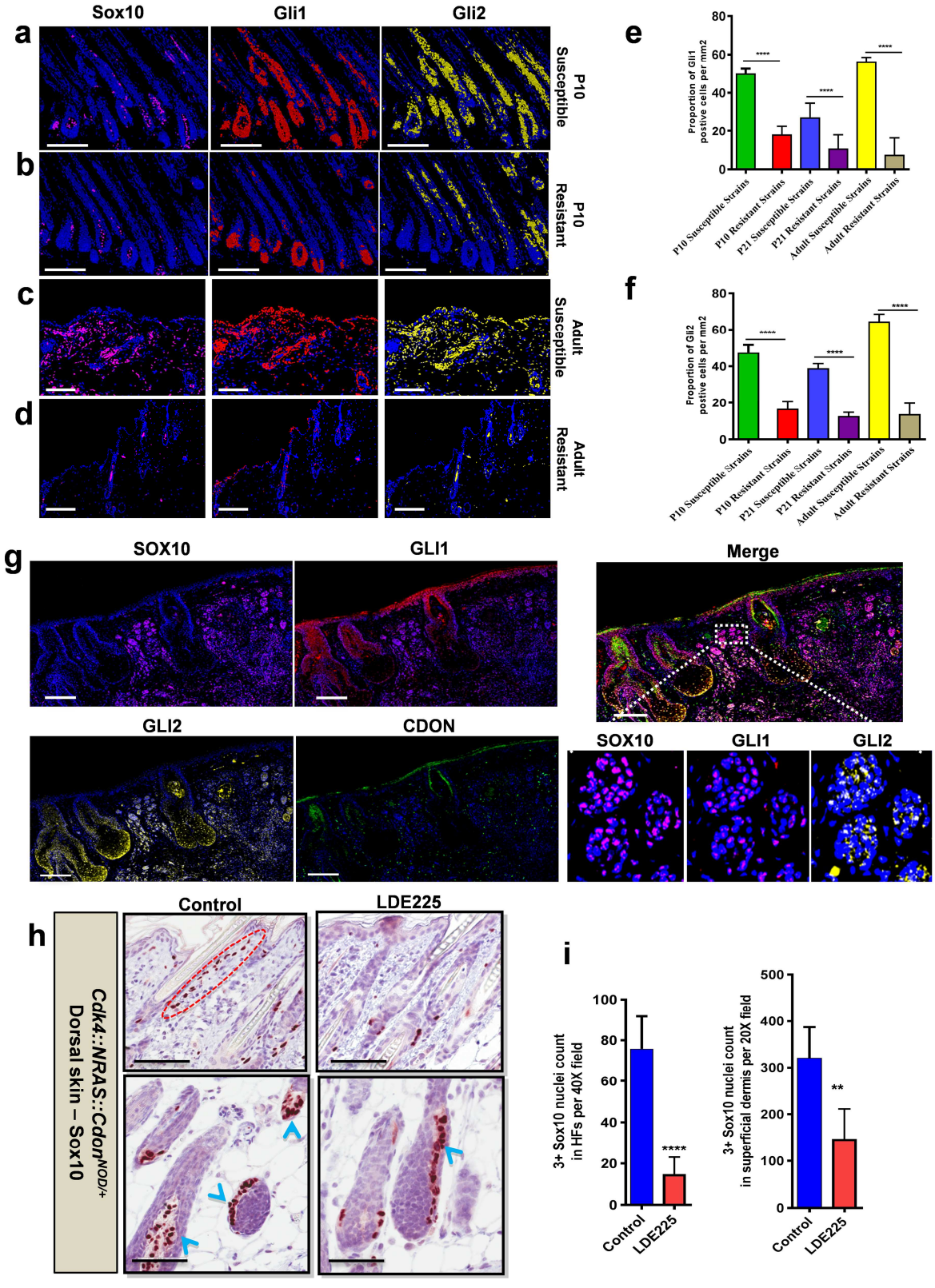
a
b
c
d
Sox10
Gli1
Gli2
P10 Susceptible
P10 Resistant
Adult Susceptible
Adult Resistant
e
Proportion of Gli1 postive cells per mm2
f
Proportion of Gli2 postive cells per mm2
P10 Susceptible Strains
P10 Resistant Strains
P21 Susceptible Strains
P21 Resistant Strains
Adult Susceptible Strains
Adult Resistant Strains
g
SOX10
GLI1
Merge
GLI2
CDON
h
Control
LDE225
Cdk4::NRAS::Cdon NOD/+
Dorsal skin – Sox10
i
3+ Sox10 nuclei count in HFs per 40X field
3+ Sox10 nuclei count in superficial dermis per 20X field

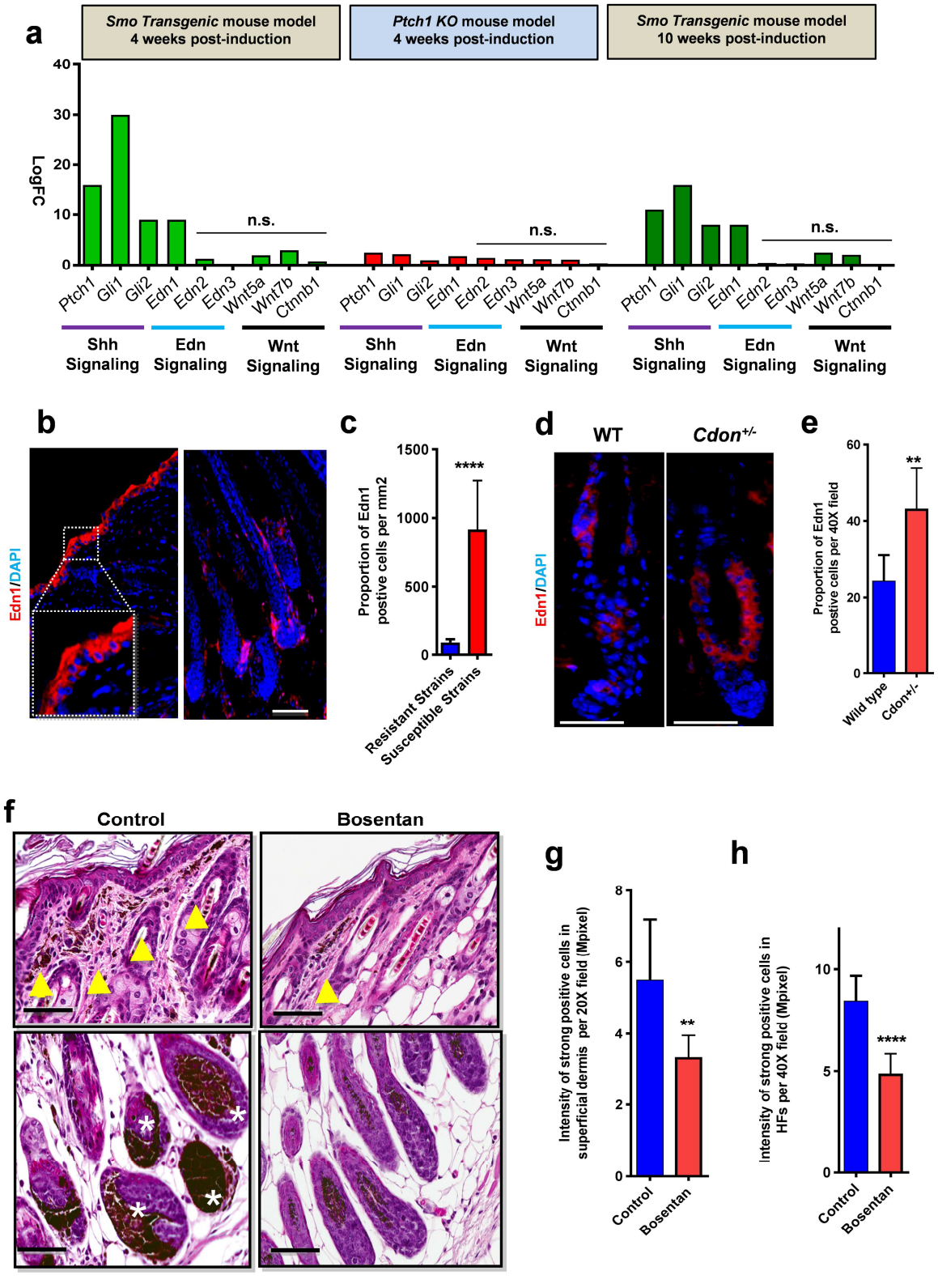
a
Smo Transgenic mouse model
4 weeks post-induction
Ptch1 KO mouse model
4 weeks post-induction
Smo Transgenic mouse model
10 weeks post-induction
LogFC
40
30
20
10
0
n.s.
n.s.
n.s.
Ptch1
Gli1
Gli2
Edn1
Edn2
Edn3
Wnt5a
Wnt7b
Ctnnb1
Shh Signaling
Edn Signaling
Wnt Signaling
b
Edn1/DAPI
c
Proportion of Edn1 postive cells per mm2
1500
1000
500
0
****
Resistant Strains
Susceptible Strains
d
WT
Cdon+/-
Edn1/DAPI
e
Proportion of Edn1 postive cells per 40X field
60
40
20
0
**
Wild type
Cdon+/-
f
Control
Bosentan
g
Intensity of strong positive cells in superficial dermis per 20X field (Mpixel)
8
6
4
2
0
**
Control
Bosentan
h
Intensity of strong positive cells in HFs per 40X field (Mpixel)
10
5
0
****
Control
Bosentan

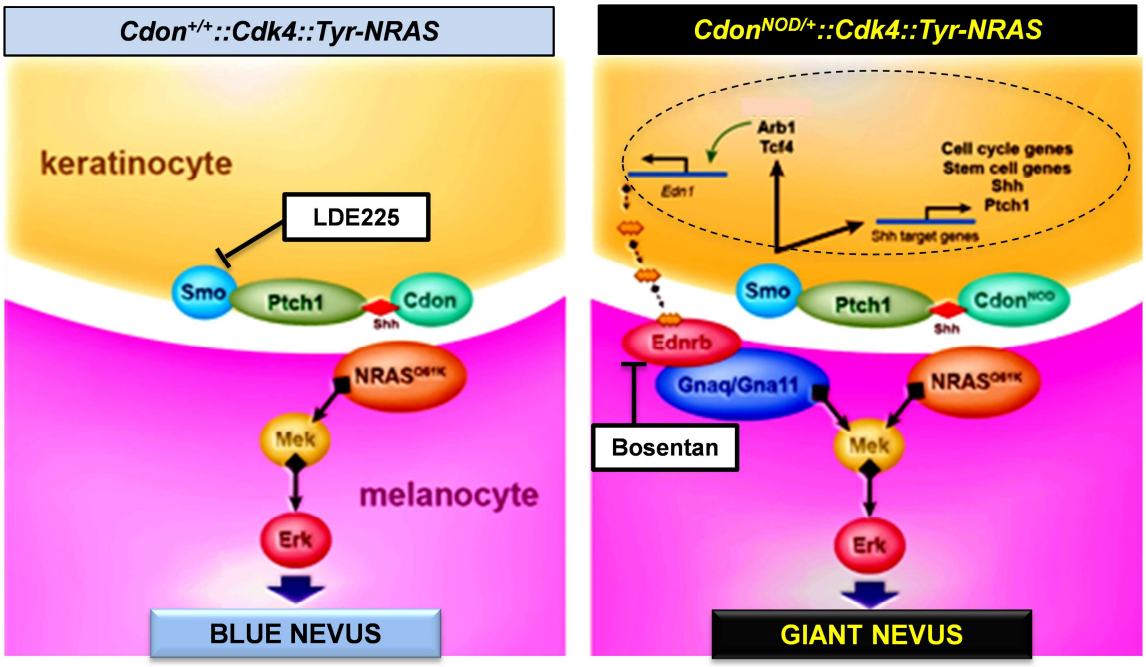
Cdon+/+::Cdk4::Tyr-NRAS
keratinocyte
LDE225
Smo
Ptch1
Cdon
Shh
NRASQ61K
Mek
Erk
melanocyte
BLUE NEVUS
CdonNOD/+::Cdk4::Tyr-NRAS
Arb1
Tcf4
Edn1
Cell cycle genes
Stem cell genes
Shh
Ptch1
Shh target genes
Smo
Ptch1
CdonNOD
Shh
Ednrb
Gnaq/Gna11
NRASQ61K
Bosentan
Mek
Erk
GIANT NEVUS